Title

Multimodular biosensors reveal a novel platform for activation of G proteins by growth factor receptors

Journal

Proceedings of the National Academy of Sciences of the United States of America, 112(9)

ISSN

0027-8424

Authors

Midde, Krishna K

Aznar, Nicolas

Laederich, Melanie B

et al.

Publication Date

2015-03-03

DOI

10.1073/pnas.1420140112

Peer reviewed

Multimodular biosensors reveal a novel platform for activation of G proteins by growth factor receptors

Krishna K. Midde[a], Nicolas Aznar[a], Melanie B. Laederich[a], Gary S. Ma[a], Maya T. Kunkel[b], Alexandra C. Newton[b], and Pradipta Ghosh[a,b,c,1]

Departments of [a]Medicine and [b]Pharmacology and [c]Moores Cancer Center, University of California, San Diego, La Jolla, CA 92093

Edited by Solomon H. Snyder, Johns Hopkins University School of Medicine, Baltimore, MD, and approved January 26, 2015 (received for review October 21, 2014)

Environmental cues are transmitted to the interior of the cell via a complex network of signaling hubs. Receptor tyrosine kinases (RTKs) and trimeric G proteins are two such major signaling hubs in eukaryotes. Conventionally, canonical signal transduction via trimeric G proteins is thought to be triggered exclusively by G protein-coupled receptors. Here we used molecular engineering to develop modular fluorescent biosensors that exploit the remarkable specificity of bimolecular recognition, i.e., of both G proteins and RTKs, and reveal the workings of a novel platform for activation of G proteins by RTKs in single living cells. Comprised of the unique modular makeup of guanidine exchange factor Gα-interacting vesicle-associated protein (GIV)/girdin, a guanidine exchange factor that links G proteins to a variety of RTKs, these biosensors provide direct evidence that RTK–GIV–Gαi ternary complexes are formed in living cells and that Gαi is transactivated within minutes after growth factor stimulation at the plasma membrane. Thus, GIV-derived biosensors provide a versatile strategy for visualizing, monitoring, and manipulating the dynamic association of Gαi with RTKs for noncanonical transactivation of G proteins in cells and illuminate a fundamental signaling event regulated by GIV during diverse cellular processes and pathophysiologic states.

heterotrimeric G protein | growth factor receptor tyrosine kinase | Girdin | PI3-kinase | Akt | invasion | cyclic AMP

The ability of cells to respond and adapt to external signals is achieved through the concerted action of several receptors and regulatory proteins. Receptor tyrosine kinases (RTKs) and G protein-coupled receptors (GPCRs) are the two most widely studied cell signaling hubs in eukaryotes. Canonical RTK signaling begins with ligand binding to the ectodomain of the receptor, leading to receptor dimerization followed by autophosphorylation of the tyrosine residues on the cytoplasmic tail and propagation of the signals to the interior of the cell via adaptor proteins (1). Canonical G protein signaling begins with ligand binding to GPCRs, which are seven transmembrane receptors with an intrinsic guanine nucleotide exchange factor (GEF) activity that enables G protein recruitment and subsequent activation through the exchange of GDP for the GTP nucleotide (2). For several decades these two pathways were believed to operate in a selective and discrete mode by transducing signals through their respective downstream intermediates. However, mounting evidence over time has unfolded a complex array of cross-talk between these two pathways, so that activated receptors from one pathway transactivate the other pathway either directly by activating the receptors (3) or indirectly by activating the downstream adaptor proteins (4). A well-documented and widely accepted phenomenon is transactivation of RTKs by GPCRs via scaffolding proteins such as β-arrestins (5). However, the reverse concept, i.e., transactivation of trimeric G proteins by RTKs, remains controversial. Despite numerous clues supporting the concept that growth factors trigger the activation of heterotrimeric G proteins (6), the fundamental question as to how such trigger occurs in cells remains poorly understood. This poorly understood concept is met with skepticism because there is no evidence that G proteins and ligand-activated RTKs come within close proximity in cells or that RTKs or any member of the growing family of signal-transducing adaptors used by RTKs can serve as GEFs. Some of these unanswered questions are being clarified by the discovery and characterization of Gα-interacting vesicle-associated protein (GIV; also known as "girdin"), an unusual signal transducer that can bind both RTKs and G proteins.

GIV is a multimodular signal transducer (Fig. 1*A*) and a GEF for Gαi (7). Working downstream of a variety of growth factors [EGF (8, 9), IGF (10), VEGF (11), insulin (7, 12, 13), and PDGF receptor (14)], GIV enhances PI3K-Akt activity, links Akt signaling to actin cytoskeleton remodeling, and triggers cell migration, all via activation of Gαi (7). Because cells can modulate incoming growth factor signals from multiple RTKs by altering the cellular levels of GIV or selectively modulating its GEF function, we likened GIV to a rheostat by which cells tune incoming signals up or down (15). Consistent with its ability to signal downstream of a variety of receptors, GIV modulates growth factor signaling during diverse biological processes (15), e.g., cell migration, chemotaxis (13), invasion (16), development (17), self-renewal (18), apoptosis (19, 20), and autophagy (12). Additionally, evidence gathered by us and others has demonstrated the clinical significance of GIV-dependent signaling during diverse disease processes, e.g., pathologic angiogenesis (11), liver fibrosis (19), diabetes (21), nephrotic syndrome (20), vascular repair (22), and tumor metastasis across a variety of cancers

Significance

Long-held tenets in the field of signal transduction are that G proteins are activated exclusively by G protein-coupled receptors and that growth factor receptor tyrosine kinases (RTKs) do not have the wherewithal to do the same. In this work we created fluorescent biosensors derived from the multimodular signal transducer Gα-interacting vesicle-associated protein (GIV), an unusual protein that binds RTKs and activates G proteins, and used them in FRET and bimolecular fluorescent complementation assays to visualize RTK–GIV–G protein signaling complexes directly in single living cells. These studies not only provide evidence that GIV serves as a platform for transactivation of G proteins by growth factor RTKs but also illuminate the spatial and temporal dynamics of such noncanonical G protein signaling.

Author contributions: K.K.M., N.A., and P.G. designed research; K.K.M., N.A., M.B.L., G.S.M., and P.G. performed research; M.T.K. and A.C.N. contributed new reagents/analytic tools; K.K.M., N.A., M.B.L., G.S.M., and P.G. analyzed data; K.K.M. and P.G. wrote the paper; and A.C.N. served as consultant for technical aspects.

The authors declare no conflict of interest.

This article is a PNAS Direct Submission.

[1]To whom correspondence should be addressed. Email: prghosh@ucsd.edu.

This article contains supporting information online at www.pnas.org/lookup/suppl/doi:10.1073/pnas.1420140112/-/DCSupplemental.

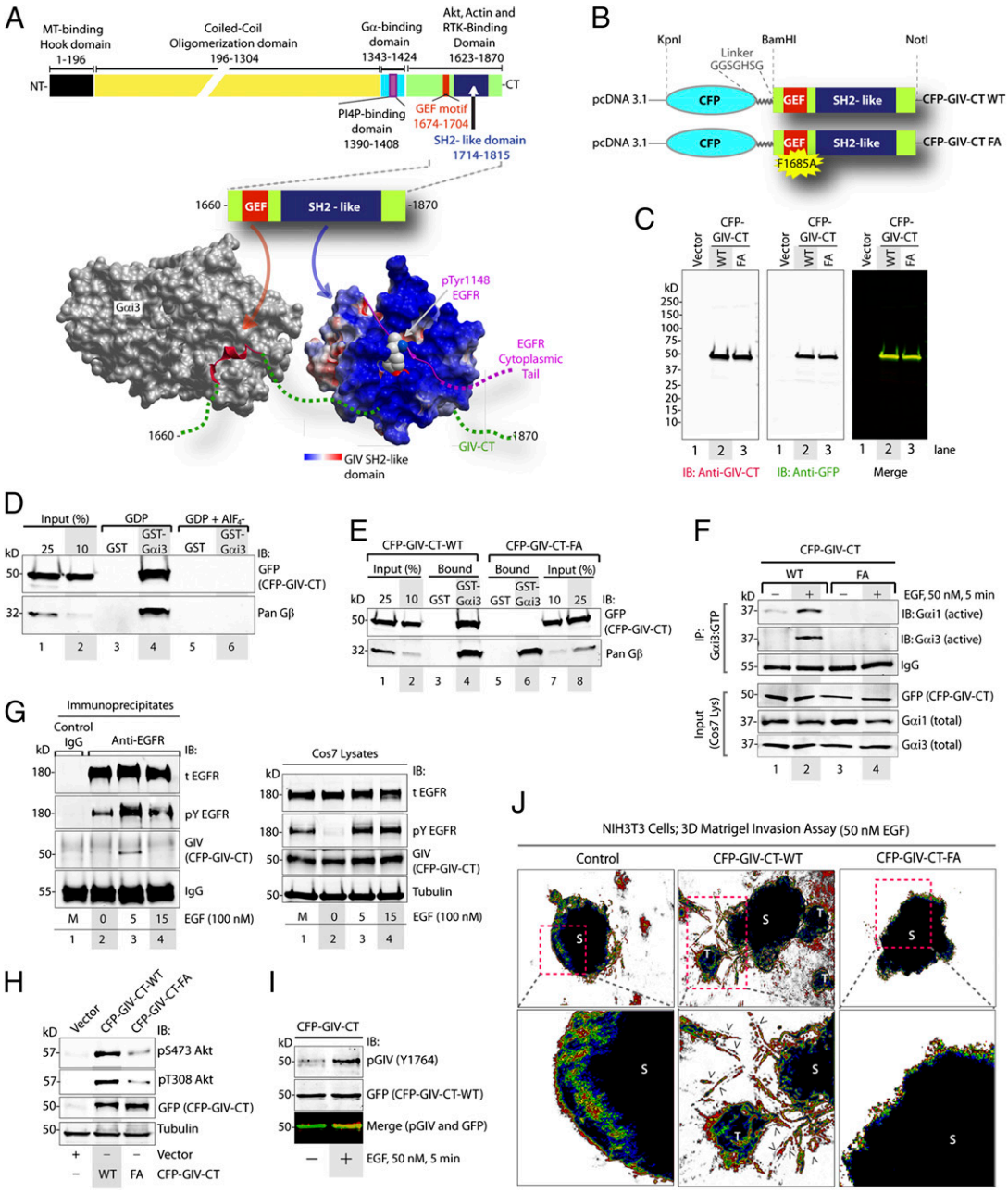

Fig. 1. Design and characterization of GIV-derived biosensors. (*A*, *Upper*) Schematic of various known functional domains of GIV. (*Lower*) The unique modular make-up of GIV's CT with in-tandem coexistence of a GEF domain (red) that activates Gαi (gray), and a SH2-like domain (blue-red) that binds autophosphorylated cytoplasmic tails of RTKs. Magenta represents EGFR pTyr peptide. The homology models displayed were validated previously (7, 28). (*B*) Schematic showing the cloning strategy used in generating CFP-tagged GIV biosensors. FA, F1685A, a previously characterized GEF-deficient mutant. (*C*) Immunoblots showing the expression of WT and FA CFP-GIV-CT biosensors in Cos7 cells. (*D*) Pulldown assay using GST-Gαi3 loaded with GDP in the presence or absence of AlF_4^- and lysates of Cos7 cells expressing CFP-GIV-CT. The positive control Gβ bound Gαi3 in the presence of GDP but not in the presence of AlF_4^-. (*E*) Pulldown assay using GST-Gαi3 loaded with GDP and lysates of Cos7 cells expressing CFP-GIV-CT-WT (lanes 1–4) or CFP-GIV-CT-FA (lanes 5–8). The positive control Gβ binds Gαi3·GDP. (*F*) Cos7 cells expressing CFP-GIV-CT-WT or -FA were starved and stimulated with EGF as indicated before lysis. Lysates were analyzed for Gαi1 and 3 activity by immunoprecipitation with anti-Gαi:GTP and immunoblotting with total Gαi1 and Gαi3 antibodies. (*G*) Cos7 cells were transfected with the GIV-CT biosensor, starved, and subsequently stimulated with EGF ligand for indicated times before lysis. EGFR-bound complexes were immunoprecipitated with anti-EGFR Ab. Immune complexes (*Left*) and lysates (*Right*) were analyzed for total EGFR (t EGFR), phosphorylated EGFR (pY EGFR), the CFP-GIV biosensor (GFP), and tubulin. M, mix of starved and EGF-stimulated lysates. (*H*) Lysates of Cos7 cells expressing CFP-GIV-CT-WT or -FA biosensors were analyzed for phosphoAkt (pS473 and pT308Akt), CFP-GIV biosensors (GFP), and tubulin. (*I*) Cos7 cells expressing the CFP-GIV-CT biosensor were starved and subsequently stimulated with EGF, and whole-cell lysates were probed for GFP and pY1764 GIV. Tyrosine phosphorylation was seen exclusively after EGF stimulation, as previously shown in the case of full-length GIV (29). (*J*, *Upper*) GIV-CT-WT, but not GIV-CT-FA, triggers cell invasion. Spheroids (S) of NIH 3T3 cells expressing CFP-GIV-CT biosensors or control vector were analyzed for their ability to invade Matrigel in response to EGF using a Cultrex-3D Spheroid Invasion Kit (Trevigen) (*SI Experimental Procedures*). Invading cells (arrowheads) and satellite tumors (T) were noted exclusively in cells expressing CFP-GIV-CT-WT. (*Lower*) Magnified views of the dashed boxes in the corresponding upper panels. Data quantification is shown in Fig. S1*B*.

[gastric (23), esophageal (24), prostate (16), breast (10, 25, 26), colon (27), and glioblastoma (18)].

Despite the accumulating information on the biological and clinical significance of GIV, how it may couple to multiple RTKs remained unknown until recently. Protein interaction assays showed that GIV's C terminus (CT) directly binds autophosphorylated cytoplasmic tails of multiple RTKs (9). Homology modeling, sequence analysis, side-chain substitution, and limited proteolysis showed that an ∼110-aa stretch within GIV's CT folds into a Scr homology 2 (SH2)-like domain and is necessary and sufficient to recognize and bind phosphotyrosine peptides (28) (Fig. 1*A*) and recruit Gαi to RTKs. The discovery of coexisting SH2-like and GEF domains in tandem within the GIV CT (Fig. 1*A*) supported the idea that GIV's CT has the necessary modular make-up to serve as a platform for linking G proteins to multiple RTKs. However, the in vitro and standard biochemical assays used thus far have failed to provide direct *in cellulo* evidence that GIV assembles RTK–GIV–Gαi ternary complexes, and if it does, when and where this assembly might occur, what might be the consequences of such assembly on G protein signaling, and how such signaling compares with the dynamics of canonical GPCR-driven G protein signaling. Such evidence would provide insights into the fundamental mechanisms that define GIV's role at the cross-roads of RTK and G protein signaling pathways in diverse pathophysiologic processes. Such findings also will imply that the evolutionarily conserved CT of GIV serves as the long-sought modular platform for transactivation of G proteins downstream of growth factors, a phenomenon that has been observed and reported by several groups over the past few decades (6).

Results and Discussion

Generation of Fluorescent Biosensors Comprised of Key Modules Derived from GIV. To visualize the formation of RTK–GIV–Gαi complexes and to gain mechanistic insights into the dynamic behavior of GIV in signal transduction, we developed multimodular fluorescent GIV biosensors. These biosensors are comprised of the CT of GIV (amino acids 1660–1870) N-terminally tagged with cyan fluorescent protein (CFP) to serve as donor (CFP-GIV-CT-WT) in FRET studies (Fig. 1 *B* and *C*). A previously described GEF-deficient mutant (7), in which Phe at position 1685 in the GEF motif is replaced by Ala (CFP-GIV-CT-FA), was created to disrupt the GIV–Gαi interaction selectively. The rationale for the design of these biosensors is multifactorial: (*i*) a complete phylogenetic analysis of GIV (15) has revealed that this stretch of GIV's CT could be functionally autonomous because it evolved independently of its N terminus (NT) (in fish), and both the NT and CT fused into full-length GIV only in birds; (*ii*) the CT contains the GEF and SH2-like domains, representing the cross-road between the GPCR/G and RTK signaling pathways; (*iii*) the CT of GIV also contains the two critical tyrosines that serve as docking sites for p85α (PI3K) (29); (*iv*) the coexistence of the GEF motif, the SH2-like domain, and the tyrosines is restricted to only the most complex of eukaryotes, i.e., mammals, and is highly conserved (∼99%) (15, 29); and (*v*) biochemical and functional assays (9) have demonstrated convincingly that the CT is the domain most critically required for GIV to carry out its functions during signal transduction downstream of RTKs. We hypothesized that the CT of GIV, which contains the GEF, the SH2-like domain, and the two critical tyrosine residues, is the minimal module that allows this region to operate autonomously and carry out most functions that previously have been attributed to full-length GIV as a signal transducer downstream of growth factor RTKs (15).

We carried out several biochemical and functional assays to determine if GIV's CT is indeed functionally autonomous. Because GIV is a GEF for Gαi1-3 subunits, but not Gαo/s (7), we first assessed the ability of GIV-CT biosensors to bind and activate Gαi. Lysates of Cos7 cells expressing CFP-tagged biosensors were used as source of GIV-CT protein in GST pulldown assays with recombinant GST-tagged Gαi3 immobilized on glutathione beads. Consistent with the known binding properties of GEFs, CFP-GIV-CT-WT preferentially bound inactive (i.e., GDP-loaded) GST-Gαi3, but not Gαi3 in active conformation (as mimicked by the presence of aluminum fluoride, AlF_4^-) (Fig. 1*D*). As anticipated, the GEF-deficient CFP-GIV-CT-FA biosensor did not bind Gαi3 (Fig. 1*E*). To determine if the GIV-CT biosensor activates Gαi in a GEF-dependent manner in Cos7 cells, we took advantage of an antibody that specifically recognizes Gαi in a GTP-bound active conformation [anti-Gαi:GTP (28, 30)]. We detected activation of Gαi1/3 in cells overexpressing the GIV-CT-WT biosensor exclusively after EGF stimulation (Fig. 1*F*), and such ligand-dependent activation was virtually abolished in cells expressing the GIV-CT-FA biosensor. We conclude that GIV-CT biosensors can bind and activate Gαi in cells in a GEF-dependent manner as previously demonstrated for full-length GIV.

Next we asked if GIV-CT biosensors are able to bind EGF receptor (EGFR) and enhance growth factor signaling. When we immunoprecipitated endogenous EGFR from Cos7 cells at various time points after EGF stimulation, the CFP-GIV-CT biosensor coimmunoprecipitated with EGFR exclusively at 5 min after ligand stimulation (Fig. 1*G*), much like our previous findings with full-length GIV (9). Consistent with the central role of GIV's GEF function in the enhancement of PI3K-Akt signals and actin remodeling (7), expression of CFP-GIV-CT-WT, but not CFP-GIV-CT-FA, maximally enhanced Akt signaling (as determined by the extent of phosphorylation of Akt at Ser-473 and Thr at 308) (Fig. 1*H*) and triggered actin remodeling (as determined by the abundance of actin stress fiber) (Fig. S1*A*). Furthermore, EGF stimulation triggered phosphorylation of the CFP-GIV-CT biosensor at a critical tyrosine, Tyr1764 (Fig. 1*I*), which is known to bind and activate PI3K directly (29). These findings demonstrate that the CFP-GIV-CT biosensors retain the properties of receptor recruitment and signal transduction characteristic of full-length GIV.

Next we asked if GIV's CT alone can reproduce complex cellular phenotypes previously attributed to full-length GIV, e.g., cell migration and invasion of basement membrane during tumor metastasis (10). To determine if the expression of CFP-GIV-CT biosensors can trigger cell invasion through basement membrane proteins, we carried out 3D Matrigel invasion assays. Noninvasive NIH 3T3 cells (31) were transfected with CFP-GIV-CT biosensors or vector control, grown into tumor spheroids, and subsequently analyzed for cell invasion in response to EGF (Fig. 1*J*). Enhanced invasion (∼3.5-fold) (Fig. S1*B*) and satellite tumors were detected exclusively in the presence of CFP-GIV-CT-WT but not in cells expressing control vector or CFP-GIV-CT-FA, indicating that GIV's CT is sufficient to trigger cell invasion and that a functionally intact GEF motif is essential. Thus, comprised of the essential modules (GEF, SH2-like, and phosphotyrosines), GIV-CT is sufficient for interaction with RTKs and G proteins, for modulation of growth factor signaling, and for triggering complex cellular processes such as cell invasion. We conclude that GIV's CT represents the smallest, functionally autonomous unit that retains many key properties of full-length GIV.

Growth Factors Trigger Interactions of GIV-CT Biosensors with EGFR and Gαi. Next we took advantage of these probes to gain insights into the workings of GIV as a signaling platform. We first visualized when and where GIV interacts with the prototype RTK EGFR and with Gαi in living cells using FRET. FRET is the principal method of choice for studying dynamic protein–protein interactions because it extends the resolution limitation of confocal microscopy (∼250 nm) to ∼10 nm and serves as a widely accepted tool for estimating the proximity of macromolecules in

living cells (32). To avoid inhomogeneities between samples, we carried out FRET imaging on single cells in a mesoscopic regime as described previously by Midde and colleagues (33, 34). To determine when and where GIV binds EGFR, Cos7 cells expressing the FRET probe pairs EGFR-YFP (35) and CFP-GIV-CT (at levels ∼1.5-twofold above endogenous GIV) were used (Fig. 2*A* and Fig. S2*A*). We found that there was no measurable FRET signal between the donor and acceptor in serum-starved cells (t0) (Fig. 2*B*). Within 5 min after EGF stimulation, CFP-GIV-CT translocated to the plasma membrane (PM) (Fig. S2*B*) where it colocalizes and interacts with EGFR, as determined by increased FRET efficiency, 0.24 ± 0.1 (Fig. 2*B*). Interaction at the PM was diminished significantly at 10 min (FRET efficiency, 0.16 ± 0.04) and was virtually abolished by 15 min after ligand stimulation. This profile of interaction was identical to that obtained using a prototype SH2 adaptor Grb2-YFP (36) and EGFR-CFP as FRET pairs in Cos7 cells (37), indicating that the dynamics of the interaction between GIV-CT and EGFR mirrors the established interaction profile of SH2 adaptors with RTKs. In these assays no such FRET was detected at any time before or after ligand stimulation when EGFR was replaced by another acceptor probe, a myristolated and palmitated YFP (a membrane-anchored fluorophore) that is known to localize to membrane microdomains that are enriched in signaling proteins (Fig. S2*C*) (38), indicating that the dynamic EGFR–GIV-CT interaction we observe is specific. We conclude that the GIV-CT biosensor behaves like other SH2 adaptors in that it is recruited to ligand-activated EGFR at the PM within 5 min and decreases rapidly thereafter. Furthermore, consistent with the previously defined role of GIV in EGFR trafficking and signaling as it transits through early endosomes (39), we noted that decreasing FRET at the PM was accompanied by the appearance of FRET on vesicular structures, presumably early endosomes. FRET was observed in these vesicles within 5–10 min before diminishing at 15 min, indicating that GIV and EGFR may continue to interact during the early steps of receptor endocytosis.

Next we asked how EGF affects the GIV–Gαi interaction in Cos7 cells expressing the FRET probe pairs CFP-GIV-CT and Gαi3-YFP, a previously well-characterized, internally tagged G protein (Fig. 2*D*) (40). Using pulldown assays, we confirmed that the internally tagged G protein was capable of binding to a GIV-CT biosensor in which CFP was replaced with GST to carry out biochemical protein–protein assays in mammalian cells. We found that YFP-tagged Gαi3 behaved like endogenous Gαi3 in Cos7 cells (Fig. S3 *A* and *B*): Both bound GIV-CT at t0 (starved state), increased maximally at 15 min after EGF stimulation, and

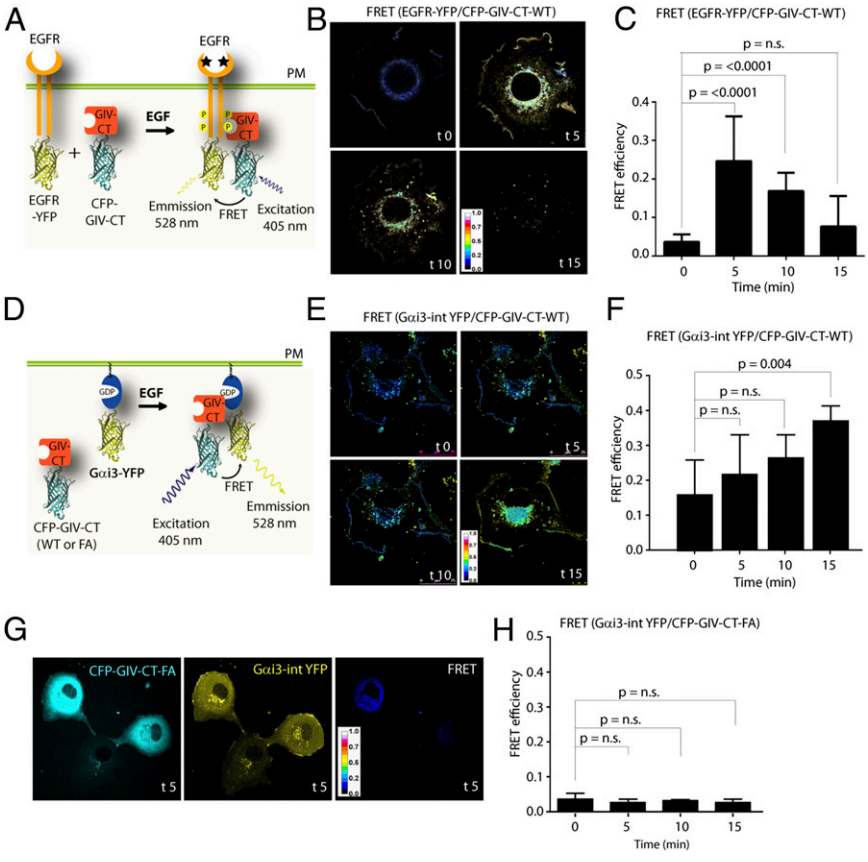

Fig. 2. FRET studies reveal dynamic interactions of GIV's CT with EGFR (*A–C*) and Gαi3 (*D–F*) in Cos7 cells. (*A*) Schematic for the EGFR and GIV-CT constructs used as paired FRET probes in *B*. (*B*) Cos7 cells were cotransfected with EGFR-YFP and CFP-GIV-CT, starved, stimulated with EGF, and analyzed for FRET (see details in *SI Experimental Procedures*). Representative freeze-frame images from live-cell movies are shown. Images show intensities of acceptor emission caused by FRET in each pixel. Maximum FRET occurred at 5 min at the PM. (*C*) Bar graphs display FRET efficiency (*y* axis) at the PM at various time points after ligand stimulation (*x* axis). Results are expressed as mean ± SD. Data represent 10 regions of interest (ROIs) analyzed over the pixels corresponding to the PM of 8–10 cells from five independent experiments. (*D*) Schematic for the GIV-CT and Gαi3 constructs used as paired FRET probes in *E*. (*E–H*) Cos7 cells expressing Gαi3 with an internal YFP tag (Gαi3-intYFP) and CFP-GIV-CT-WT (*E* and *F*) or CFP-GIV-CT-FA (*G* and *H*) were ligand stimulated and analyzed as in *B*. Images show intensities of acceptor emission caused by FRET in each pixel. FRET between Gαi3-YFP and CFP-GIV-CT-WT occurred at the PM at t0 and increased significantly at t15 min. (*F*) Bar graphs display FRET efficiency (*y* axis) at the PM at various time points after ligand stimulation (*x* axis) analyzed as in *C*. Results are expressed as mean ± SD. (*G* and *H*) No FRET was observed between Gαi3-YFP and the GEF-deficient CFP-GIV-CT-FA probe at any time point after EGF stimulation.

declined significantly by 30 min. FRET imaging revealed that Gαi3-YFP acceptor and CFP-GIV-CT-WT donor probes interacted at the PM both before (t 0) and after ligand stimulation and that maximal interaction at the PM occurred by 15 min (FRET efficiency, 0.36 ± 0.004) (Fig. 2 *D* and *F*). Although the majority of cells analyzed showed peak interaction between GIV and Gαi3 at the PM at 15 min, we noted that in a few cells this peak was achieved rapidly, within ∼5 min (Fig. S3*C*). These findings indicate that although some starved cells preassemble GIV–Gαi complexes at steady state, presumably for immediate use early during receptor activation, others assemble the complexes in a ligand-dependent manner. The GIV–Gαi complexes assembled later (at ∼15 min after ligand stimulation) may trigger the activation of G proteins on signaling endosomes as ligand-activated receptors traffic through those compartments, as has been demonstrated recently in the case of canonical GPCR/G protein signaling (41). Regardless of the timing of assembly, most of these GIV–Gαi complexes disassemble at ∼30 min after ligand stimulation (Fig. S3 *A* and *B*), as is consistent with our previous finding that a negative feedback loop initiated at that time by PKCθ triggers phosphorylation of GIV's GEF motif at Ser1689 which selectively terminates GIV's ability to bind or activate Gαi (14). Furthermore, consistent with the previously described abundance of Gαi3 and GIV at the Golgi (13, 42, 43), we observed FRET/interaction between the probes on a perinuclear compartment. No interaction either at the PM or on internal membranes was observed at any time before or after ligand stimulation when we used the GEF-deficient CFP-GIV-CT-FA mutant biosensor that cannot bind Gαi (Fig. 2 *G* and *H*). These biochemical and biophysical studies provide direct evidence that GIV-CT interacts with Gαi3 at the PM, where it interacts with ligand-activated EGFR 5 min after ligand stimulation, indicating that GIV-CT biosensors may assemble and allow visualization of ternary EGFR–GIV–Gαi3 complexes at the PM.

GIV-CT Biosensors Serve as Platforms for Assembling RTK–GIV–Gαi Ternary Complexes at the PM. To detect the ligand-dependent formation of RTK–GIV–Gαi ternary complexes at the PM, we took advantage of another approach widely used to study protein–protein interactions, bimolecular fluorescence complementation (BiFC) (44, 45), and used it in combination with FRET. In this approach, the interaction between two macromolecules (i.e., GIV-CT and EGFR) is detected by BiFC, and the interaction with the third partner (i.e., Gαi3) is monitored by FRET. Although the BiFC approach previously has been used independently to study GPCR oligomerization (46) and the interaction of SH2 adaptor proteins with EGFR (47), and FRET has been used extensively to study both RTK and GPCR/G protein pathways, there is no precedence for their use in combination (BiFC-FRET) to study growth factor/G protein signaling pathways. We tagged the GIV-CT biosensor with the NT of Venus (VN; 173 residues) (VN-GIV-CT) and fused the CT of Venus (VC; 85 residues) to the cytoplasmic tail of EGFR for use in BiFC assays (Fig. 3*A*). Immunoblots and biochemical assays confirmed that all BiFC constructs are expressed in Cos7 cells as intact proteins of the expected size without proteolytic fragments (Fig. 3*B*) and that VN-GIV-CT biosensors retain their ability to bind inactive Gαi3 (Fig. S4*A*) in a GEF-dependent manner (Fig. S4*B*). When coexpressed with EGFR-VC, both VN-GIV-CT-WT and -FA could interact with the receptor, as determined by the yellow fluorescence observed at the PM and on vesicles, presumably endosomes, in all transfected cells (Fig. 3*C*, *Bottom*). This pattern of fluorescence resembled that observed previously in BiFC studies using VN-growth factor receptor-bound protein 2 (Grb2) and EGFR-VC (47). None of the cells expressing VN and VC or either in combination with EGFR-VC or VN-GIV-CT showed any fluorescence (Fig. 3*C*, *Top* and *Middle*), indicating that in the absence of interacting proteins the NT or CT fragments of Venus alone are incapable of fluorescence complementation. Because we previously showed that such complementary fluorescence requires a functionally intact SH2-like domain in GIV (28), the fluorescence complementation we observe in cells coexpressing EGFR-VC and VN-GIV-CT indicates that EGFR–GIV complexes were assembled via the SH2-like domains of both WT and FA biosensors and visualized by BiFC.

To visualize the formation of RTK–GIV–Gαi ternary complexes, we used Cos7 cells coexpressing the BiFC probes (EGFR-VC and VN-GIV-CT) and internally tagged Gαi3-CFP. When these cells were stimulated with EGF, FRET was observed from donor Gαi3-CFP to acceptor Venus-tagged EGFR–GIV complexes (assembled by BiFC probes) at the PM within 5 min (Fig. 4*A* and Movie S1), indicating that ligand stimulation triggers the assembly of EGFR–GIV–Gαi complexes in cells. These complexes continued to interact at the PM until 10 min and thereafter disassembled within 15 min after EGF stimulation. No such FRET was observed at any time before or after ligand stimulation when the GIV–Gαi3 interaction was disrupted selectively using either of the two previously described mutants: a GEF-deficient VN-GIV-CT-FA mutant (7) biosensor as a BiFC probe to assemble EGFR–GIV complexes (Fig. 4 *B* and *C*) and a Gαi3-CFP W258F (WF) mutant that does not bind GIV (48) as a FRET probe (Fig. 4 *C* and *D*, Fig. S5, and Movie S2). These results provide direct evidence that EGFR–GIV–Gαi3 ternary complexes are assembled at the PM after ligand stimulation and that interaction between GIV and Gαi3 is essential for the assembly of such ternary complexes. Because an intact SH2-like domain of GIV is essential for fluorescence complementation between EGFR and GIV-CT BiFC probes (28), assembly of EGFR–GIV–Gαi3 complexes by BiFC-FRET requires two functionally intact modules within the GIV-CT biosensors—a GEF motif to bind Gαi3 and a SH2-like domain to bind ligand-activated EGFR (Fig. 1*A*). Because ternary complexes were assembled at the PM exclusively between 5 and 10 min after ligand stimulation, unlike the GIV–Gαi complexes, which were in part preformed and in part ligand-induced (with a delayed peak at ∼15 min) (Fig. 2 *D* and *E*), it is likely that the rapid assembly of ternary complexes within 5 min at the PM is contributed largely by the preformed GIV–Gαi complexes.

RTKs Interact with Gαi and Trigger Their Noncanonical Activation via GIV. A critical question was whether GIV-dependent assembly of RTK–GIV–Gαi ternary complexes at the PM functionally links RTKs to G protein signaling. We used GIV-depleted or control Cos7 cells expressing the FRET probe pairs EGFR-CFP (35) and Gαi3-YFP to measure ligand-dependent complex formation (Fig. 5*A*). Compared with control cells, in which ligand stimulation triggers the assembly of EGFR–GIV–Gαi3 complexes at the PM, we anticipated that such complexes do not assemble in the GIV-depleted cells. FRET imaging revealed that EGFR and Gαi3 interact (FRET efficiency, 0.25) at the PM within 5 min after ligand stimulation in control cells (Fig. 5 *B* and *D* and Movie S3). The two FRET probes continued to interact at the PM up to 10 min, but by 15 min such interaction was virtually undetectable (Fig. 5 *B* and *D*), mirroring the dynamics of interaction we observed for EGFR and GIV (Fig. 2 *A*–*C*) and EGFR–GIV–Gαi3 ternary complexes (Fig. 4*A*). No such interaction was observed before or after ligand stimulation in GIV-depleted cells (FRET efficiency, 0.013) (Fig. 5 *C*–*E* and Movie S4), demonstrating that GIV is required for Gαi3 to come within close proximity of ligand-activated EGFR. To determine if this requirement holds true for other members of the RTK superfamily, we studied the insulin receptor (InsR), a class II RTK that is closely related to EGFR (a class I RTK) but differs significantly in structural and functional aspects (49). We previously showed that the GEF function of GIV modulates critical insulin metabolic signaling programs (12). As seen in the case of EGFR, when control cells coexpressing Gαi3-YFP and a previously

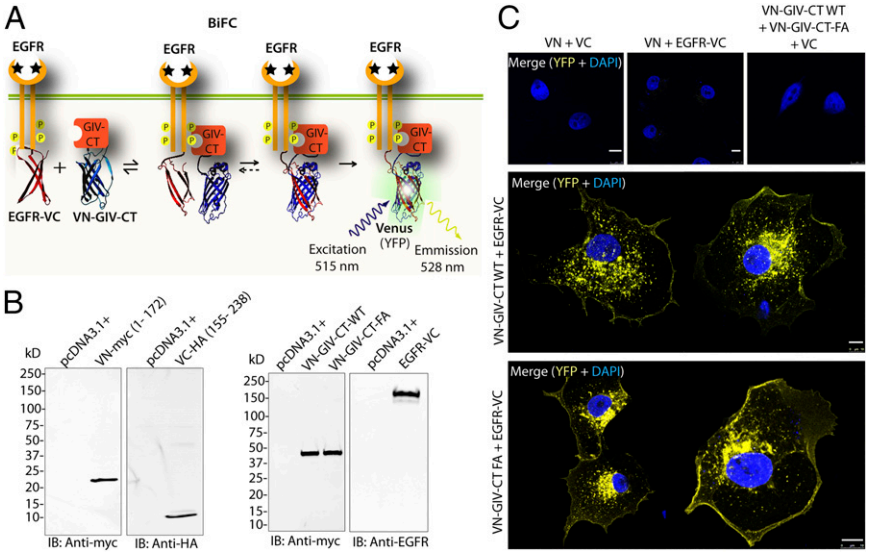

Fig. 3. Visualization of EGFR–GIV complexes using BiFC. (*A*) Schematic for the EGFR-VC and VN-GIV-CT constructs used as BiFC probes in *B* and *C*. (*B*) Immunoblots showing expression of VN, VC, EGFR-VC, and VN-GIV-CT probes in Cos7 cells. (*C*) Cos7 cells were cotransfected with VC + VN, EGFR-VC + VN-GIV-CT-WT, or EGFR-VC + VN-GIV-CT-FA, and the formation of the bimolecular fluorescent Venus (YFP) complex was assessed by confocal imaging. Both WT and FA BiFC probes interacted with EGFR-VC at the PM and with endosomes at steady state.

characterized InsRβ-CFP (50) were stimulated with insulin, interaction between Gαi3 and InsRβ was observed at the PM at 5 min (FRET efficiency, 0.27 ± 0.07) (Fig. 5 *F* and *H*). However, such interaction was reduced significantly in GIV-depleted cells (FRET efficiency, 0.13 ± 0.02) (Fig. 5 *G* and *H*), indicating that the role of GIV in facilitating the proximity between

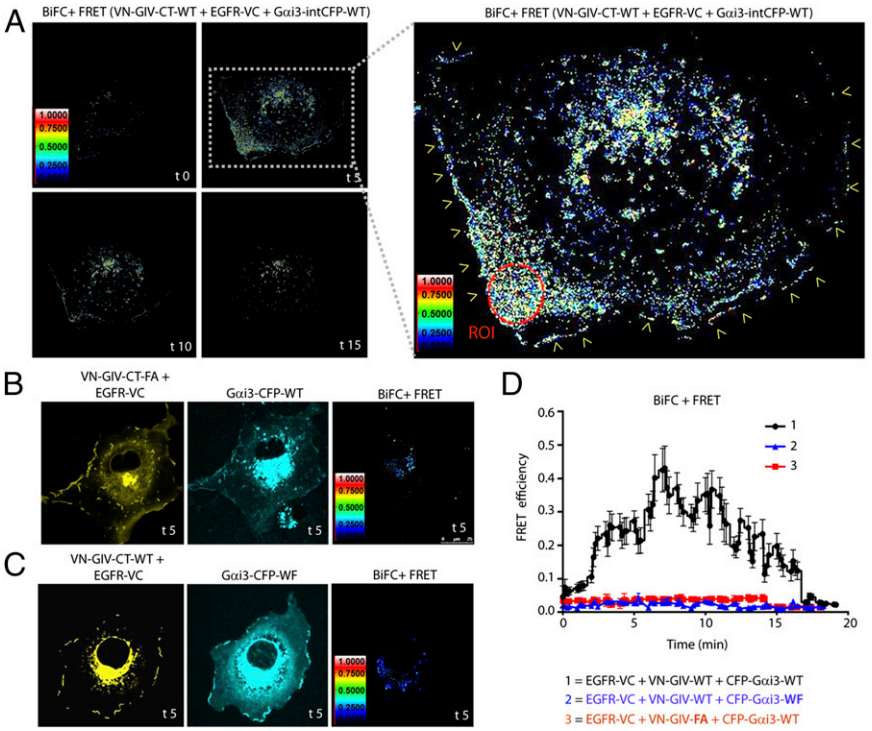

Fig. 4. Visualization of EGFR–GIV–Gαi ternary complexes using a combination of BiFC and FRET. (*A*, *Left*) Cos7 cells were cotransfected with EGFR-VC and VN-GIV-CT-WT BiFC probes and CFP-Gαi3-WT, starved, and stimulated with EGF. EGFR–GIV–Gαi3 ternary complexes were visualized at the PM by FRET imaging. Representative freeze-frame images from live-cell movies are shown, which display the intensities of acceptor emission caused by FRET in each pixel. Maximum FRET occurred at 5 min (t5) at the PM. (*Right*) Higher magnification of the area in the white dashed box in t5. A representative ROI is shown in the red circle. (*B*) Cos7 cells were cotransfected with EGFR-VC and VN-GIV-CT-FA BiFC probes and CFP-Gαi3-WT, starved, and stimulated with EGF. No energy transfer was seen at the PM. (*C*) Cos7 cells were cotransfected with EGFR-VC and VN-GIV-CT-WT BiFC probes and CFP-Gαi3-WF, starved, and stimulated with EGF. No energy transfer was seen at the PM. (*D*) Time-traces of changes in FRET intensity after stimulation with EGF ligand in Cos7 cells transfected with various BiFC and FRET probes in *A*–*C*. Data are shown as mean ± SD; n = 10 ROIs from three independent experiments.

ligand-activated RTKs and Gαi is not limited to one RTK but most likely is a fundamental phenomenon that couples Gαi to multiple RTKs (7, 15).

To eliminate the possibility that GPCRs somehow may play a role in bringing the G proteins in close proximity to RTKs, we carried out FRET imaging using EGFR-CFP and a Gαi3 protein tagged at its CT with YFP. Previous studies have established that a tag at that position on a G protein effectively uncouples it from GPCRs and abrogates downstream signaling via adenylyl cyclase/cyclic AMP (cAMP) (51). We found that the GPCR-insensitive Gαi3-YFP(CT) probe also interacts with EGFR-CFP at the PM within 5 min after EGF stimulation (FRET efficiency ∼0.25 ± 0.04) (Fig. S6), indicating that the interaction between EGFR and Gαi3 shown in Fig. 5*B* is not dependent on signaling cross-talk with GPCRs. Next we analyzed if endogenous EGFR and Gαi3 come in close proximity of each other in Cos7 cells after ligand stimulation using direct stochastic optical reconstruction microscopy (dSTORM) imaging. STORM achieves a spatial resolution of ∼25 nm in the lateral dimensions and ∼50 nm in the axial dimension and allows visualization of endogenous proteins

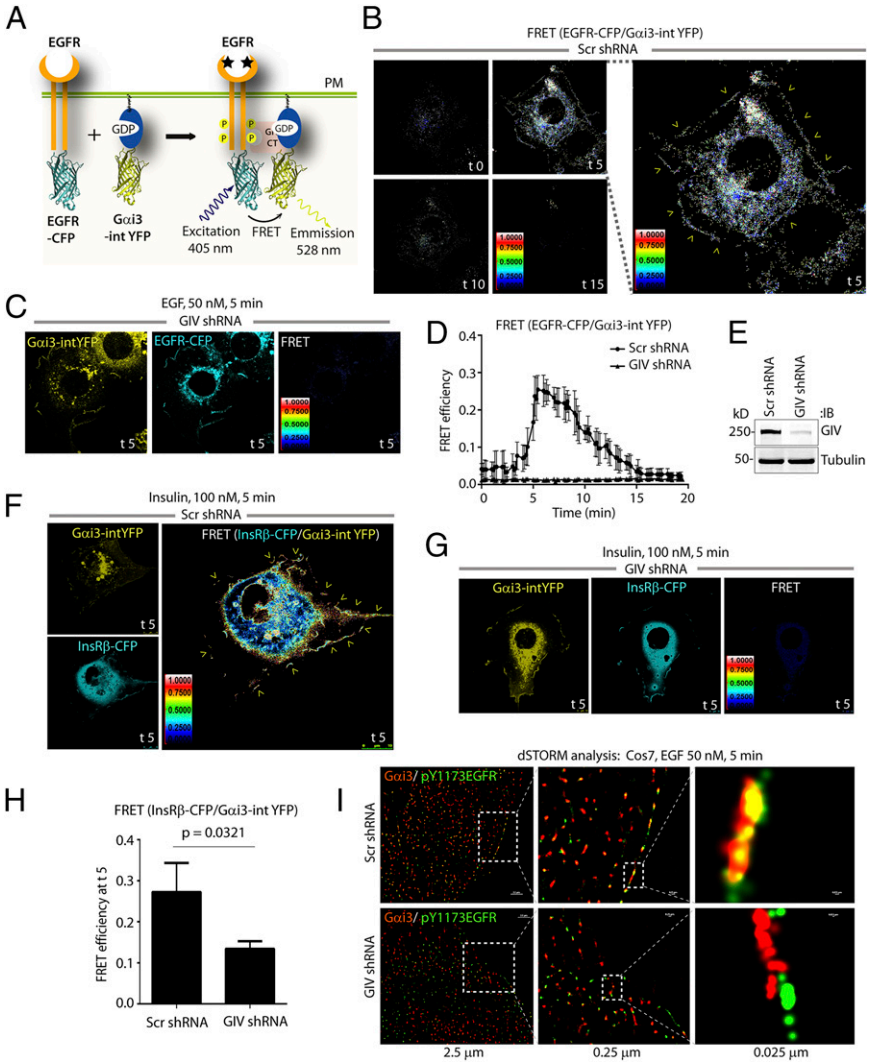

Fig. 5. The CT of GIV is sufficient to facilitate interaction between ligand-activated EGFR and Gαi3. (*A*) Schematic for the EGFR and Gαi3 constructs used as paired FRET probes. (*B* and *C*) Control [Scramble (Scr) shRNA] (*B*) or GIV-depleted (GIV shRNA) (*C*) Cos7 cells were cotransfected with EGFR-YFP and Gαi3-intCFP, starved, stimulated with EGF, and analyzed for FRET by live-cell confocal microscopy. (*B*, *Left*) Representative freeze-frame images from live-cell movies of control (Scr shRNA) Cos7 cells, which display intensities of acceptor emission caused by FRET in each pixel. Ligand-dependent maximal interaction of the donor and acceptor probes occurs at 5 min at the PM. (*Right*) The freeze-frame image at t5 shown at higher magnification. (*C*) Representative freeze-frame YFP, CFP, and FRET images of GIV-depleted cells at t5. No FRET is seen at the PM. (*D*) Time-traces of changes in FRET efficiency after stimulation with EGF in control (Scr shRNA) and GIV-depleted (GIV shRNA) Cos7 cells cotransfected with various BiFC and FRET probes. Data are shown as mean ± SD; $n = 10$ ROIs from three independent experiments. Interaction of the donor and acceptor probes was observed in Scr shRNA-treated cells but not in GIV-depleted cells. (*E*) Cos7 cells stably expressing shRNA against GIV or Scr (control) were lysed and analyzed for efficient depletion of GIV by immunoblotting. Efficacy of GIV depletion as determined by band densitometry was ∼95% or greater. (*F* and *G*) Control (Scr shRNA) (*F*) or GIV-depleted (GIV shRNA) (*G*) Cos7 cells were cotransfected with InsRβ-CFP and Gαi3-intYFP and subsequently were ligand stimulated and analyzed as in *B* and *C*. Images display CFP, YFP, and intensities of acceptor emission caused by FRET in each pixel at t5. Interaction of the donor and acceptor probes was observed in Scr shRNA-treated cells but not in GIV-depleted cells. (*H*) Bar graphs display differences between FRET intensities observed in Scr shRNA vs. GIV-depleted cells in *F* and *G*, respectively. Error bars represent mean ± SD. The analysis represents five ROIs from four or five cells from three independent experiments. (*I*) Starved and EGF-stimulated Cos7 cells were fixed and stained for endogenous ligand-activated autophosphorylated EGFR (pY1173EGFR) (green) and Gαi3 (red) and were analyzed by dSTORM microscopy. Colocalization (yellow pixels) was observed at the PM in merged images of control cells (*Upper*) but not of GIV-depleted cells (*Lower*).

in situ; the high degree of colocalization observed between proteins indicates that they are likely to interact (52). We visualized endogenous G protein using anti-Gαi3 pAb and the ligand-activated pool of EGFR using anti-pY1173 mAb because this autophosphorylation event serves as one of the major sites for recruitment of GIV's SH2-like domain (28). A high degree of colocalization was observed along the PM (Fig. 5*I*, yellow pixels) in EGF-stimulated control Cos7 cells but not in GIV-depleted cells, demonstrating that native forms of ligand-activated RTKs and Gαi come within close proximity of each other exclusively in the presence of GIV. We conclude that (*i*) ligand-activated RTKs come within close proximity of Gαi at the PM, where they are likely to interact; (*ii*) GIV is required to facilitate such interactions; and (*iii*) this phenomenon occurs independently without input from GPCRs.

To investigate if the close proximity of RTKs to Gαi proteins affects the activation status of the latter, we used a widely accepted approach in which activation of trimeric Gi is monitored by the dissociation of fluorescent-tagged Gαi and Gβγ subunits with a resultant loss of FRET (53–55) (Fig. 6*A*). When control

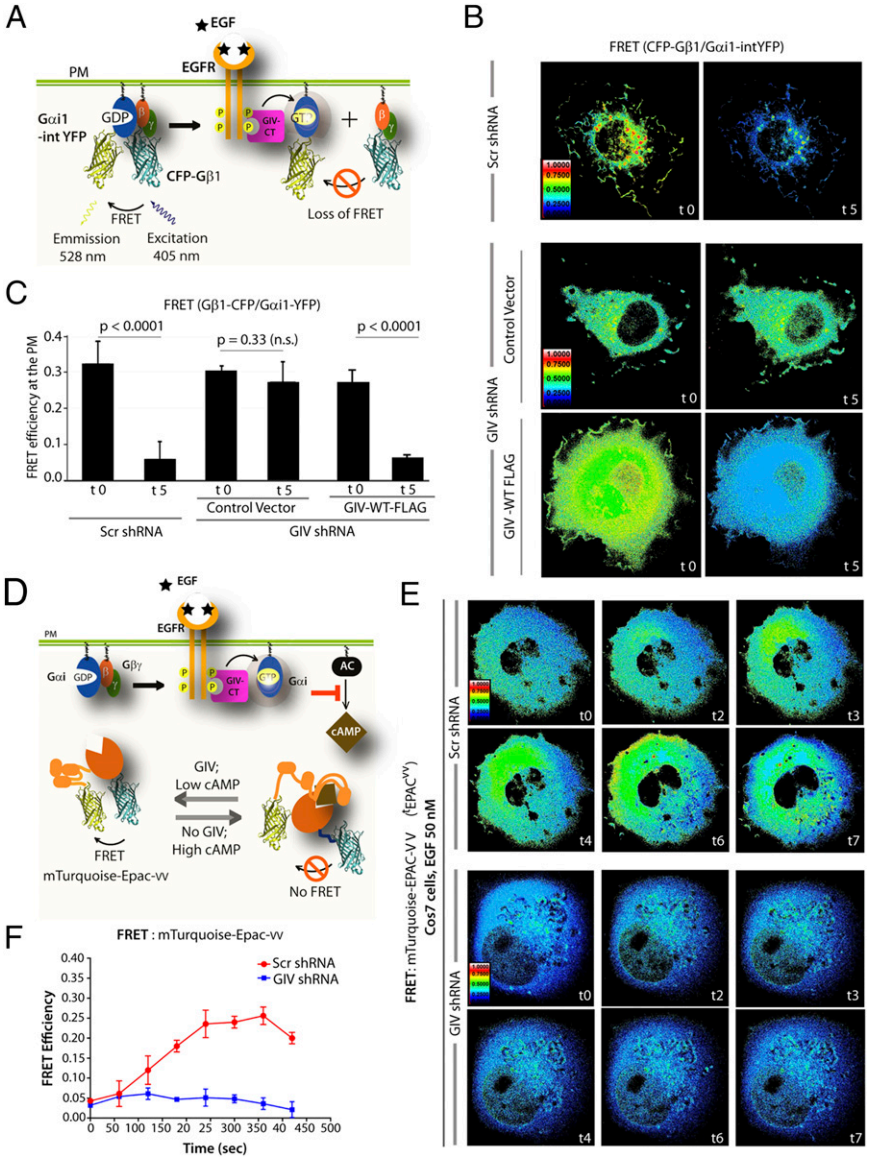

Fig. 6. GIV is required for the transactivation of Gi proteins in response to growth factors. (*A*) Schematic for the Gαi1-intYFP and CFP-Gβ1 constructs used as paired FRET probes in *B*. (*B*) Control (Scr shRNA) (*Left*) or GIV-depleted (GIV shRNA) (*Right*) Cos7 cells were cotransfected with Gαi3-intYFP, CFP-Gβ1, and Gγ2 with or without GIV-WT-FLAG, as indicated, and subsequently were ligand stimulated and analyzed as in Fig. 5*B*. Images show intensities of acceptor emission caused by FRET in each pixel at t5. Activation of Gi, as determined by the loss of interaction (i.e., FRET) between Gαi and Gβγ, was observed exclusively after ligand stimulation (compare t0 and t5) in control but not in GIV-depleted Cos7 cells. Activation of Gi was restored after GIV-depleted cells were transfected with shRNA-resistant GIV-WT. (*C*) Bar graphs display changes in FRET efficiency at the PM observed in *B*. Error bars represent mean ± SD. The analysis represents five ROIs from four or five cells from three independent experiments. (*D*) Schematic for the mTurquoise-EPAC-Venus ($^{T}EPAC^{VV}$) construct used as a FRET probe for measuring dynamic changes in cellular cAMP in response to EGF in *E*. (*E*) Control (Scr shRNA) (*Upper*) or GIV-depleted (GIV shRNA) (*Lower*) Cos7 cells were transfected with $^{T}EPAC^{VV}$, starved, stimulated with EGF, and analyzed for FRET by live-cell confocal microscopy. Representative freeze-frame FRET images of cells at indicated time points are shown. EGF suppressed cAMP in control but not in GIV-depleted cells, as determined by an increase in intramolecular FRET with the $^{T}Epac^{VV}$ probe. Similar results were observed when carried out in the presence of Forskolin. (*F*) Time-traces of changes in FRET efficiency after stimulation with EGF in *E*. Data are shown as mean ± SD; n = 10 ROIs from three independent experiments.

Cos7 cells coexpressing Gαi3-YFP (internal tag), CFP-Gβ_1 (NT tag), and Gγ_2 were stimulated with EGF, we observed dissociation of the Gi heterotrimer at the PM within 5 min as determined by a drop in FRET efficiency from 0.32 to 0.057 (Fig. 6 *B* and *C*), indicating that Gi is activated in response to EGF. In contrast, in GIV-depleted cells, FRET between the donor CFP-Gβγ and acceptor Gαi-YFP subunits at the PM continued with similar efficiency before and after EGF stimulation, indicating that Gi heterotrimers remained intact and that Gαi remained inactive. Activation of Gi was restored in GIV-depleted cells by exogenously expressing shRNA-resistant GIV-WT, as determined by a drop in FRET efficiency from 0.27 to 0.066 (Fig. 6 *B* and *C*). These results demonstrate that GIV is essential for the transactivation of Gi downstream of EGFR, to an extent similar to that reported previously (54) in response to U.K.14304, an agonist for α2-adrenergic receptor (i.e., an ∼25% loss of FRET efficiency). Next we assessed cellular levels of cAMP using a previously well-characterized mTurquoise- exchange protein activated by cAMP (EPAC)-Venus (^{T}Epac^{VV}) FRET probe that detects submicromolar changes in the second messenger (Fig. 6*D*) (56). We found that in the presence of GIV (control cells), transactivation of Gi by EGFR also is accompanied by transient suppression of cellular cAMP in response to EGF, as determined by the increase in intramolecular FRET (Fig. 6*E* and Movie S5). The peak FRET signal, i.e., maximal suppression of cAMP, was observed at ∼5–6 min (Fig. 6*F*), an event that is delayed significantly compared with the rapid (i.e., within seconds) suppression observed with the same FRET probes in the setting of canonical activation of Gi by Gi-coupled GPCRs (57). However, in the absence of GIV (GIV-depleted cells) no suppression of cAMP was observed in response to EGF (Fig. 6 *E* and *F* and Movie S6). We conclude that one of the immediate consequences of the RTK–GIV–Gαi complexes is activation of Gαi and suppression of levels of cAMP in close proximity to ligand-activated RTKs.

Conclusions

These findings challenge the long-standing paradigm in signal transduction that activation of G proteins is triggered exclusively by GPCRs and that RTKs do not have the wherewithal to trigger such activation. Our work establishes that RTKs indeed can interact with and activate G proteins using GIV as a platform for cross-talk. This study also unravels the spatial and temporal aspects of noncanonical transactivation of heterotrimeric Gi proteins by ligand-activated RTKs. Although the extent of Gi activation downstream of RTKs (EGFR; this work) and GPCRs (α2 AR) (54) appear similar, canonical activation of G proteins by GPCRs occurs rapidly (i.e., within milliseconds) (58), whereas noncanonical transactivation of G proteins by RTKs is both delayed and sustained (i.e., starts at ∼5 min and lasts 5–10 min). Delayed activation of Gi and suppression of cAMP are consistent with the dynamics of binding of GIV's SH2-like domain to ligand-activated RTKs, and such binding is a prerequisite step which facilitates the proximity between G proteins and RTKs.

Our findings also suggest that GIV-CT biosensors, which are comprised of RTK-binding SH2-like and G protein-activating GEF modules in tandem (Fig. 1*A*), may be used more generally as a versatile strategy to detect a variety of RTK–GIV–Gαi complexes in living cells. By the same token, the dominant negative GEF-deficient mutant biosensors that inhibit the formation of RTK–GIV–Gαi complexes offer a strategy for inhibiting aberrant signaling via this pathway. These strategies provide the foundation for the development of other genetic and nongenetic approaches for understanding key biological roles of the GIV platform that sets up crosstalk between growth factor RTKs and G proteins and for exogenous manipulation of the RTK–GIV–Gi signaling pathway in diverse diseases driven by GIV-GEF.

Experimental Procedures

Detailed methods are provided in *SI Experimental Procedures*.

Protocols for FRET studies and information on the constructs used here are detailed in *SI Experimental Procedures*. Briefly, an Olympus FV1000 inverted confocal laser scanning microscope was used for live-cell FRET imaging at the University of California, San Diego Neuroscience Core Facility. To optimize the signal-to-noise ratio in FRET imaging, various expression levels of the transfected FRET probes were tested. However, to minimize complexities arising from molecular crowding, FRET probes were overexpressed by ∼1.5- to twofold compared with the endogenous proteins. Because the stoichiometry of FRET probes has a significant impact on FRET efficiency, cells that expressed equimolar amounts of donor and acceptor probes (as determined by computing the intensity of the fluorescence signal by a photon-counting histogram) were chosen selectively for FRET analyses.

ACKNOWLEDGMENTS. We thank Jennifer Santini for assistance with FRET imaging studies, which were performed at the University of California, San Diego (UCSD) Neuroscience Microscopy Shared Facility (supported by NIH Grant P30 NS047101), Kersi Pestonjamasp for assistance with STORM microscopy at UCSD Moores Cancer Center Microscopy Shared Facility (supported by NIH Grant P30 CA23100), and Marilyn Farquhar, Irina Kufareva, and Gordon Gill for thoughtful comments during the preparation of this paper. This work was funded by National Institutes of Health (NIH) Grants R01CA160911 and R01 DK099226, the Burroughs Wellcome Fund, Doris Duke Charitable Foundation (DDCF) Clinical Scientist Developmental Award 2010058, and American Cancer Society Grant ACS-IRG 70-002 (to P.G.). G.S.M. was supported by DDCF Grant 2013073 (to P.G.) and A.C.N. and M.T.K. were supported by NIH Grant P01 DK054441 (to A.C.N.).

1. Schlessinger J (2014) Receptor tyrosine kinases: Legacy of the first two decades. *Cold Spring Harb Perspect Biol* 6:a008912.
2. Gilman AG (1987) G proteins: Transducers of receptor-generated signals. *Annu Rev Biochem* 56:615–649.
3. Daub H, Weiss FU, Wallasch C, Ullrich A (1996) Role of transactivation of the EGF receptor in signalling by G-protein-coupled receptors. *Nature* 379(6565):557–560.
4. Natarajan K, Berk BC (2006) Crosstalk coregulation mechanisms of G protein-coupled receptors and receptor tyrosine kinases. *Methods Mol Biol* 332:51–77.
5. Pierce KL, Luttrell LM, Lefkowitz RJ (2001) New mechanisms in heptahelical receptor signaling to mitogen activated protein kinase cascades. *Oncogene* 20(13):1532–1539.
6. Marty C, Ye RD (2010) Heterotrimeric G protein signaling outside the realm of seven transmembrane domain receptors. *Mol Pharmacol* 78(1):12–18.
7. Garcia-Marcos M, Ghosh P, Farquhar MG (2009) GIV is a nonreceptor GEF for G alpha i with a unique motif that regulates Akt signaling. *Proc Natl Acad Sci USA* 106(9): 3178–3183.
8. Enomoto A, et al. (2005) Akt/PKB regulates actin organization and cell motility via Girdin/APE. *Dev Cell* 9(3):389–402.
9. Ghosh P, et al. (2010) A Galphai-GIV molecular complex binds epidermal growth factor receptor and determines whether cells migrate or proliferate. *Mol Biol Cell* 21(13):2338–2354.
10. Jiang P, et al. (2008) An actin-binding protein Girdin regulates the motility of breast cancer cells. *Cancer Res* 68(5):1310–1318.
11. Kitamura T, et al. (2008) Regulation of VEGF-mediated angiogenesis by the Akt/PKB substrate Girdin. *Nat Cell Biol* 10(3):329–337.
12. Garcia-Marcos M, Ear J, Farquhar MG, Ghosh P (2011) A GDI (AGS3) and a GEF (GIV) regulate autophagy by balancing G protein activity and growth factor signals. *Mol Biol Cell* 22(5):673–686.
13. Ghosh P, Garcia-Marcos M, Bornheimer SJ, Farquhar MG (2008) Activation of Galphai3 triggers cell migration via regulation of GIV. *J Cell Biol* 182(2):381–393.
14. López-Sánchez I, et al. (2013) Protein kinase C-theta (PKCθ) phosphorylates and inhibits the guanine exchange factor, GIV/Girdin. *Proc Natl Acad Sci USA* 110(14): 5510–5515.
15. Ghosh P, Garcia-Marcos M, Farquhar MG (2011) GIV/Girdin is a rheostat that fine-tunes growth factor signals during tumor progression. *Cell Adhes Migr* 5(3):237–248.
16. Dunkel Y, et al. (2012) STAT3 protein up-regulates Gα-interacting vesicle-associated protein (GIV)/Girdin expression, and GIV enhances STAT3 activation in a positive feedback loop during wound healing and tumor invasion/metastasis. *J Biol Chem* 287(50):41667–41683.
17. Ohara K, et al. (2012) Involvement of Girdin in the determination of cell polarity during cell migration. *PLoS ONE* 7(5):e36681.
18. Natsume A, et al. (2012) Girdin maintains the stemness of glioblastoma stem cells. *Oncogene* 31(22):2715–2724.
19. Lopez-Sanchez I, et al. (2014) GIV/Girdin is a central hub for profibrogenic signalling networks during liver fibrosis. *Nat Commun* 5:4451.
20. Wang H, et al. (2014) GIV/Girdin Links Vascular Endothelial Growth Factor Signaling to Akt Survival Signaling in Podocytes Independent of Nephrin. *J Am Soc Nephrol* 26(2):314–327.

21. Hartung A, et al. (2013) The Akt substrate Girdin is a regulator of insulin signaling in myoblast cells. *Biochim Biophys Acta* 1833(12):2803–2811.
22. Miyake H, et al. (2011) The actin-binding protein Girdin and its Akt-mediated phosphorylation regulate neointima formation after vascular injury. *Circ Res* 108(10): 1170–1179.
23. Wang C, Lin J, Li L, Wang Y (2014) Expression and clinical significance of girdin in gastric cancer. *Mol Clin Oncol* 2(3):425–428.
24. Shibata T, et al. (2013) Girdin, a regulator of cell motility, is a potential prognostic marker for esophageal squamous cell carcinoma. *Oncol Rep* 29(6):2127–2132.
25. Jin F, Liu C, Guo Y, Chen H, Wu Y (2013) Clinical implications of Girdin and PI3K protein expression in breast cancer. *Oncol Lett* 5(5):1549–1553.
26. Ling Y, et al. (2011) Clinical implications for girdin protein expression in breast cancer. *Cancer Invest* 29(6):405–410.
27. Garcia-Marcos M, et al. (2011) Expression of GIV/Girdin, a metastasis-related protein, predicts patient survival in colon cancer. *FASEB J* 25(2):590–599.
28. Lin C, et al. (2014) Structural basis for activation of trimeric Gi proteins by multiple growth factor receptors via GIV/Girdin. *Mol Biol Cell* 25(22):3654–3671.
29. Lin C, et al. (2011) Tyrosine phosphorylation of the Gα-interacting protein GIV promotes activation of phosphoinositide 3-kinase during cell migration. *Sci Signal* 4(192): ra64.
30. Lane JR, et al. (2008) Antibodies that identify only the active conformation of G(i) family G protein alpha subunits. *FASEB J* 22(6):1924–1932.
31. Albini A, et al. (1987) A rapid in vitro assay for quantitating the invasive potential of tumor cells. *Cancer Res* 47(12):3239–3245.
32. Lakowicz JR (2006) *Principles of Fluorescence Spectroscopy* (Springer, New York), 3rd Ed.
33. Borejdo J, Rich R, Midde K (2012) Mesoscopic analysis of motion and conformation of cross-bridges. *Biophys Rev* 4(4):299–311.
34. Midde K, et al. (2014) Membrane topology of human presenilin-1 in SK-N-SH cells determined by fluorescence correlation spectroscopy and fluorescent energy transfer. *Cell Biochem Biophys* 70(2):923–932.
35. Pennock S, Wang Z (2008) A tale of two Cbls: Interplay of c-Cbl and Cbl-b in epidermal growth factor receptor downregulation. *Mol Cell Biol* 28(9):3020–3037.
36. Yamazaki T, et al. (2002) Role of Grb2 in EGF-stimulated EGFR internalization. *J Cell Sci* 115(Pt 9):1791–1802.
37. Sorkin A, McClure M, Huang F, Carter R (2000) Interaction of EGF receptor and grb2 in living cells visualized by fluorescence resonance energy transfer (FRET) microscopy. *Curr Biol* 10(21):1395–1398.
38. Zacharias DA, Violin JD, Newton AC, Tsien RY (2002) Partitioning of lipid-modified monomeric GFPs into membrane microdomains of live cells. *Science* 296(5569): 913–916.
39. Beas AO, et al. (2012) Gαs promotes EEA1 endosome maturation and shuts down proliferative signaling through interaction with GIV (Girdin). *Mol Biol Cell* 23(23): 4623–4634.
40. Bünemann M, Frank M, Lohse MJ (2003) Gi protein activation in intact cells involves subunit rearrangement rather than dissociation. *Proc Natl Acad Sci USA* 100(26): 16077–16082.
41. Murphy JE, Padilla BE, Hasdemir B, Cottrell GS, Bunnett NW (2009) Endosomes: A legitimate platform for the signaling train. *Proc Natl Acad Sci USA* 106(42): 17615–17622.
42. Weiss TS, et al. (2001) Galpha i3 binding to calnuc on Golgi membranes in living cells monitored by fluorescence resonance energy transfer of green fluorescent protein fusion proteins. *Proc Natl Acad Sci USA* 98(26):14961–14966.
43. Le-Niculescu H, Niesman I, Fischer T, DeVries L, Farquhar MG (2005) Identification and characterization of GIV, a novel Galpha i/s-interacting protein found on COPI, endoplasmic reticulum-Golgi transport vesicles. *J Biol Chem* 280(23):22012–22020.
44. Shyu YJ, Suarez CD, Hu CD (2008) Visualization of ternary complexes in living cells by using a BiFC-based FRET assay. *Nat Protoc* 3(11):1693–1702.
45. Hynes TR, Yost EA, Yost SM, Berlot CH (2011) Multicolor BiFC analysis of G protein βγ complex formation and localization. *Methods Mol Biol* 756:229–243.
46. Vidi PA, Przybyla JA, Hu CD, Watts VJ (2010) Visualization of G protein-coupled receptor (GPCR) interactions in living cells using bimolecular fluorescence complementation (BiFC). *Current Protocols in Neuroscience* (John Wiley & Sons, Inc., NJ)Chapter 5:Unit 5 29.
47. Liu S, Li X, Yang J, Zhang Z (2014) Low false-positives in an mLumin-based bimolecular fluorescence complementation system with a bicistronic expression vector. *Sensors (Basel)* 14(2):3284–3292.
48. Garcia-Marcos M, Ghosh P, Ear J, Farquhar MG (2010) A structural determinant that renders G alpha(i) sensitive to activation by GIV/girdin is required to promote cell migration. *J Biol Chem* 285(17):12765–12777.
49. Ward CW, Garrett TP (2004) Structural relationships between the insulin receptor and epidermal growth factor receptor families and other proteins. *Curr Opin Drug Discov Devel* 7(5):630–638.
50. Uhles S, Moede T, Leibiger B, Berggren PO, Leibiger IB (2003) Isoform-specific insulin receptor signaling involves different plasma membrane domains. *J Cell Biol* 163(6): 1327–1337.
51. Sheridan DL, et al. (2002) A new way to rapidly create functional, fluorescent fusion proteins: Random insertion of GFP with an in vitro transposition reaction. *BMC Neurosci* 3:7.
52. Huang B, Babcock H, Zhuang X (2010) Breaking the diffraction barrier: Super-resolution imaging of cells. *Cell* 143(7):1047–1058.
53. Janetopoulos C, Jin T, Devreotes P (2001) Receptor-mediated activation of heterotrimeric G-proteins in living cells. *Science* 291(5512):2408–2411.
54. Gibson SK, Gilman AG (2006) Gialpha and Gbeta subunits both define selectivity of G protein activation by alpha2-adrenergic receptors. *Proc Natl Acad Sci USA* 103(1): 212–217.
55. Yi TM, Kitano H, Simon MI (2003) A quantitative characterization of the yeast heterotrimeric G protein cycle. *Proc Natl Acad Sci USA* 100(19):10764–10769.
56. Klarenbeek JB, Goedhart J, Hink MA, Gadella TW, Jalink K (2011) A mTurquoise-based cAMP sensor for both FLIM and ratiometric read-out has improved dynamic range. *PLoS ONE* 6(4):e19170.
57. Ponsioen B, et al. (2004) Detecting cAMP-induced Epac activation by fluorescence resonance energy transfer: Epac as a novel cAMP indicator. *EMBO Rep* 5(12): 1176–1180.
58. Ross EM (2008) Coordinating speed and amplitude in G-protein signaling. *Curr Biol* 18(17):R777–R783.